Electronic Supplementary Material (ESI) for Sustainable Energy & Fuels.
This journal is © The Royal Society of Chemistry 2022

Supporting information for

$Co_xNi_{1-x}O$-$NiCo_2O_4$/rGO Synergistic Bifunctional Electrocatalysts for High-Rate Rechargeable Zinc-Air Battery

Zixuan Huang, Mai Thanh Nguyen,* Wei Jian Sim, Masayuki Takahashi, Soorathep Kheawhom, Tetsu Yonezawa*
Email: mai_nt@eng.hokudai.ac.jp, tetsu@eng.hokuai.ac.jp

Number of Figures: 15

Table of content

Estimation of electron transfer number using K-L plot based on LVS obtained from ORR electrochemical test

All of the potentials in the paper have been converted to the potential versus the reversible hydrogen electrode (RHE) according to the equation:

$$E_{vs}RHE = E_{vs}Hg/HgO + E_{\emptyset}Hg/HgO + 0.059pH \qquad (1)$$

The electron transfer number was calculated by Koutecky-Levich plots (K-L plots)according to Koutecky-Levich equation:

$$\frac{1}{J} = \frac{1}{J_K} + \frac{1}{J_L} = \frac{1}{J_K} + \frac{1}{B_{\omega^{1/2}}} \qquad (2)$$

$$B = 0.62nFC_0(D_0)^{2/3}\nu^{-1/6} \qquad (3)$$

$$J_K = nFkC_0 \qquad (4)$$

In which ω is the angular velocity, J is the current density measured in the electrochemical test, J_K and J_L are the kinetic-limiting and diffusion-limiting current densities, respectively, F is the Faraday constant of 96485 C mol^{-1}, D_0 is the diffusion coefficient, where for O_2 is 1.65×10^{-3} cm^2 s^{-1}, v is the kinematic viscosity of the electrolyte, which is 0.95×10^{-2} cm^2 s^{-1}, C_0 is the bulk concentration, where for O_2 is 0.83×10^{-6} mol cm^{-3} and n is the electron transfer number.

B can be obtained by the slope of K-L plots, and then n can be calculated. [1, 2]

Estimation of "x" in $Co_xNi_{1-x}O$ bimetallic oxides

The mole fraction, x, of Co (vs Co+Ni) in $Co_xNi_{1-x}O$ of CoNi/rGO-2/8 to 6/4 was calculated by the peak position belonged to (200) plane of $Co_xNi_{1-x}O$ based on Vegard's law and (200) XRD peak position of $Co_xNi_{1-x}O$, CoO, and NiO.

The XRD peak position of (200) plane of CoO and NiO according to the reference located at 42.388 ° and 43.280 °, respectively.

The (200) peak position detected by XRD for $Co_xNi_{1-x}O$ located at m °.

Then, according to Vegard's law, the x value in $Co_xNi_{1-x}O$ can be obtained by:

$$x \times 42.388 + (1 - x) \times 43.280 = m$$

$$\text{Thus, } x = \frac{43.280 - m}{0.892}$$

Estimation of molar ratio of $Co_xNi_{1-x}O$ bimetallic oxide and spinel $NiCo_2O_4$ phase

Co:Ni molar feeding ratios of CoNi/rGO-i/j samples is as Co:Ni = i:j (mol/mol)

In the CoNi/rGO product, the molar ratio of $Co_xNi_{1-x}O$:$NiCo_2O_4$ = f:g (mol:mol).

Assuming the reaction was completed with only two products ($Co_xNi_{1-x}O$ and $NiCo_2O_4$) and spinel $NiCo_2O_4$ exists in its stoichiometric form, the conservation of mole gives us:

Mole of Co: $fx + 2g = i$

And mole of Ni: $f(1 - x) + g = j$

Thus, $f = \frac{i-2j}{3x-2}$ and $g = \frac{(i+j)x-i}{3x-2}$

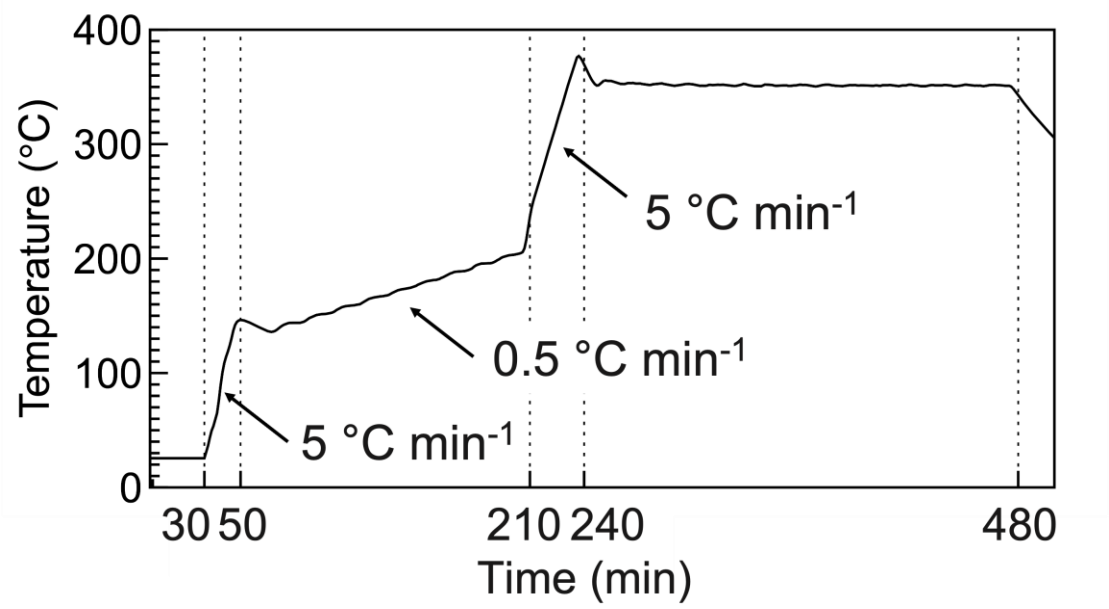

Figure S1. Temperature profile for the synthesis of CoNi/rGO catalysts.

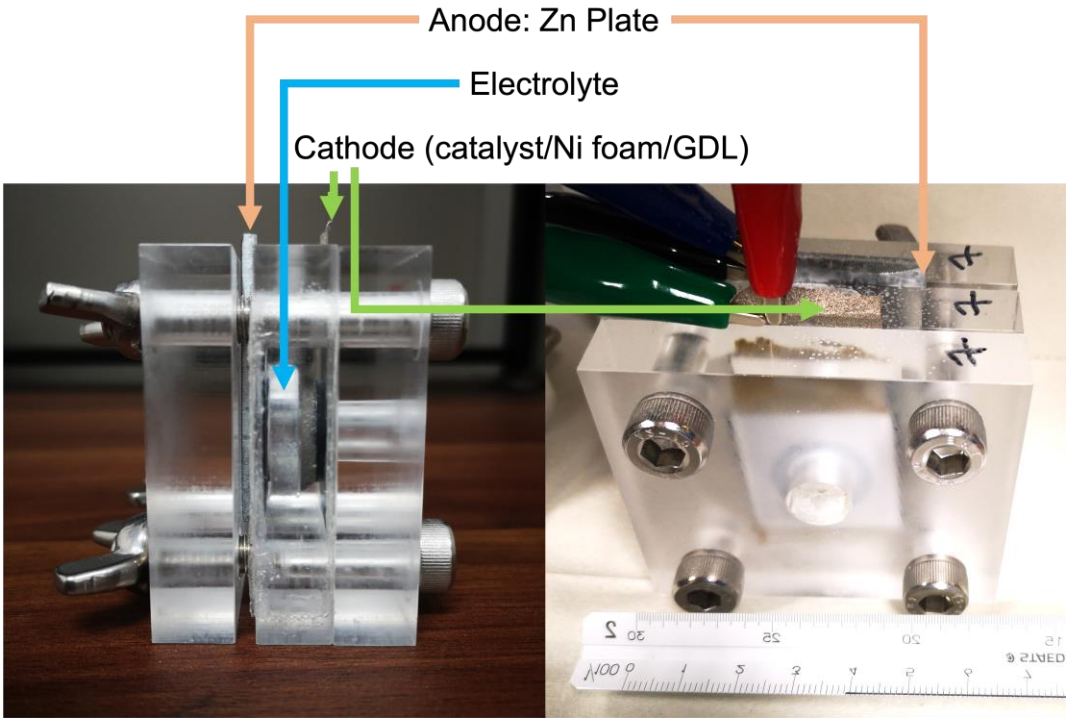

Figure S2. Photo of the ZAB cell used in the battery test.

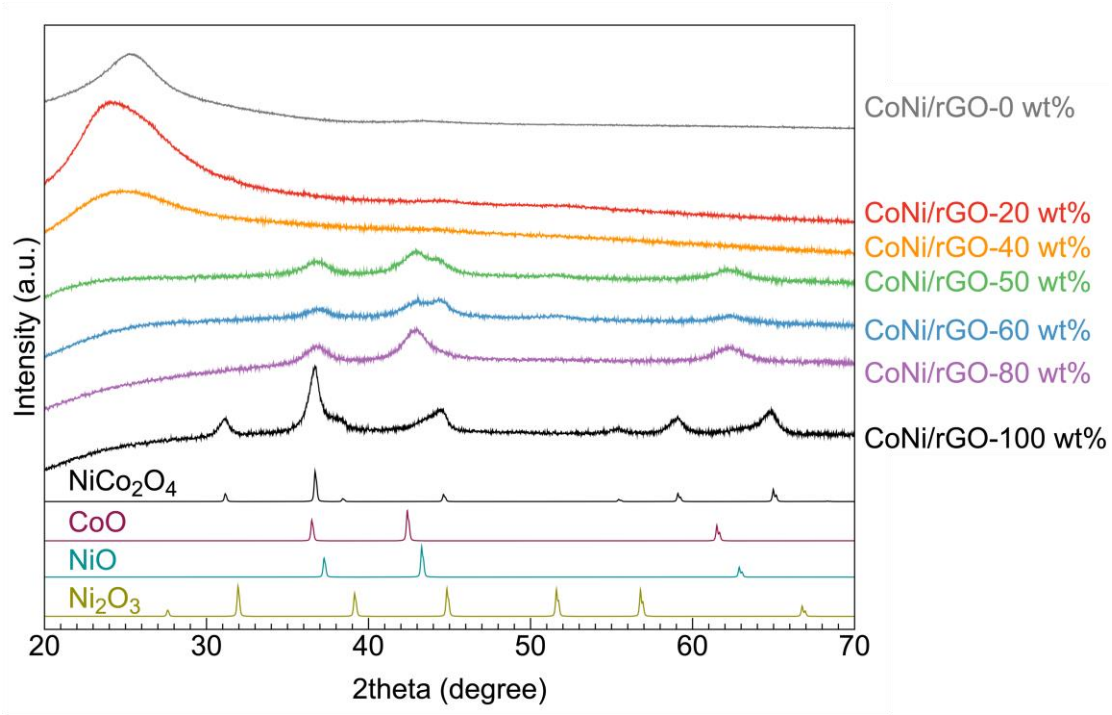

Figure S3. XRD patterns of the as-prepared CoNi/rGO samples with different metal loading amounts of 0-100 wt%. The standard patterns of $NiCo_2O_4$ (JCPDS No. 00-020-0781), CoO (JCPDS No. 00-048-1719), NiO (JCPDS No. 00-047-1049), and Ni_2O_3 (JCPDS No. 00-014-0481) are shown at the bottom of the figure.

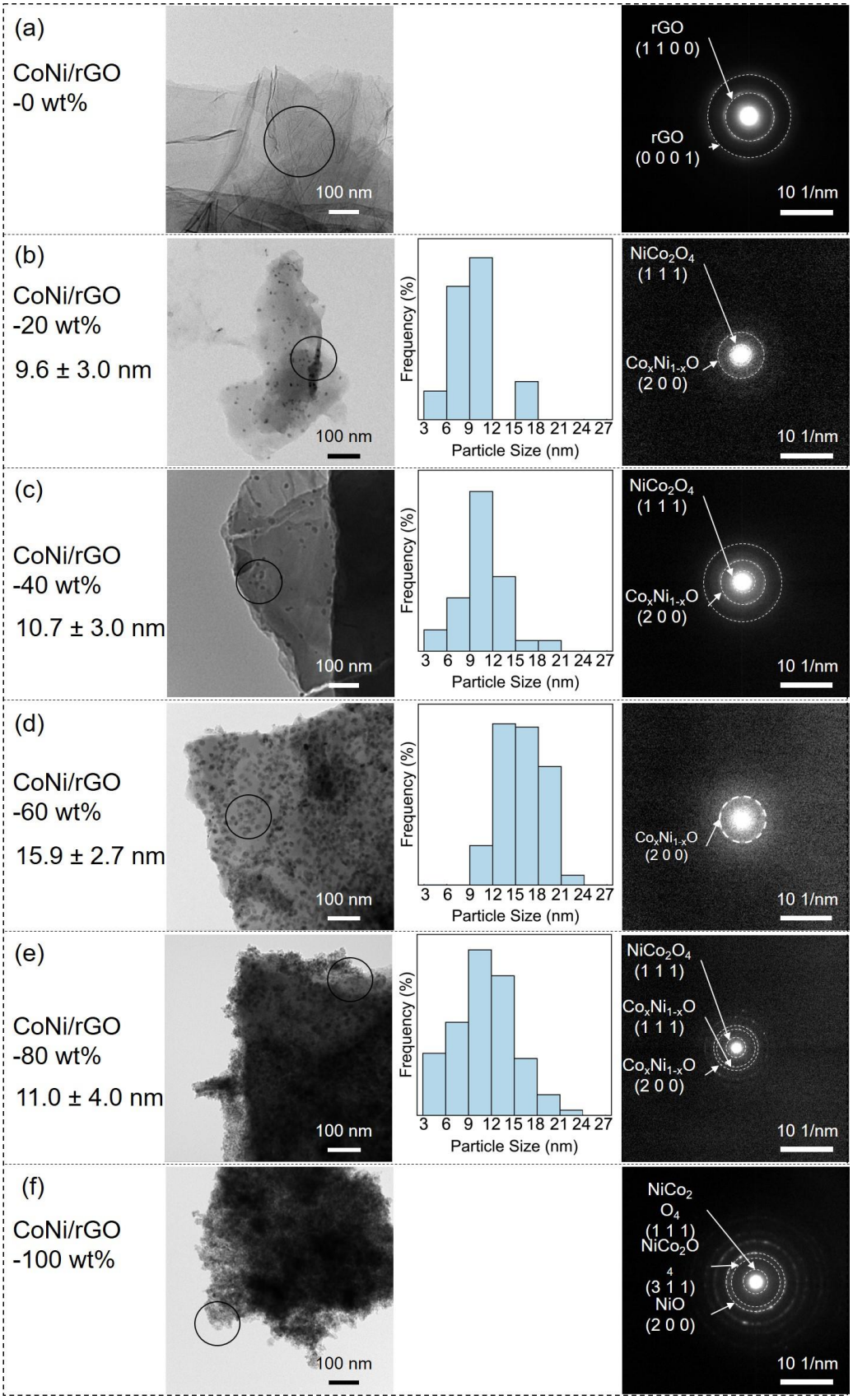

Figure S4. (left to right) TEM images, size distributions, and SAED patterns of CoNi/rGO with metal loading of (a) 0, (b) 20, (c) 40, (d) 60, (e) 80, and (f) 100 wt %.

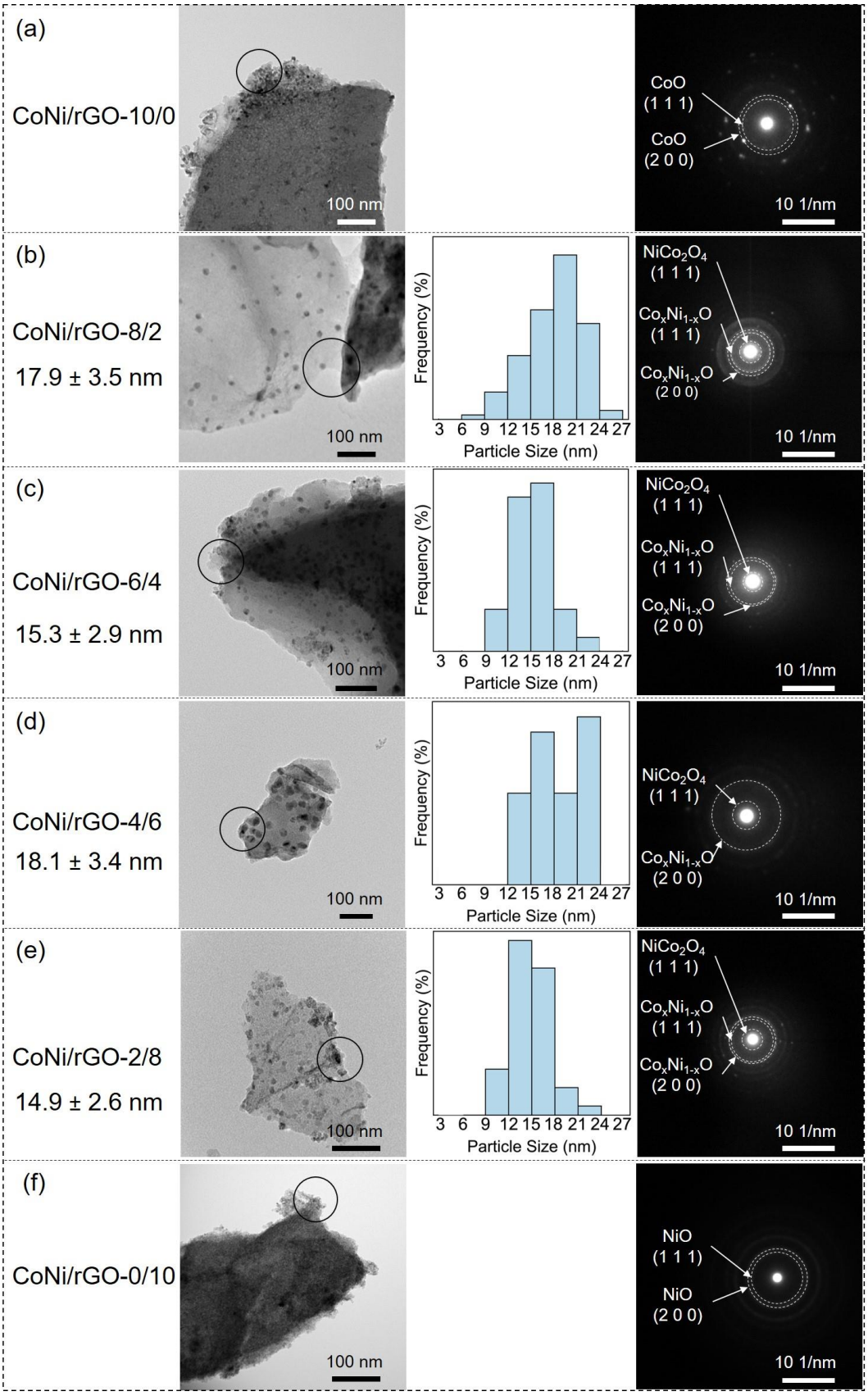

Figure S5. (left to right) TEM images, size distributions, and SAED patterns of CoNi/rGO-i/j with Co:Ni = (a) 10/0, (b) 8/2, (c) 6/4, (d) 4/6, (e) 2/8, and (f) 0/10 (mol/mol).

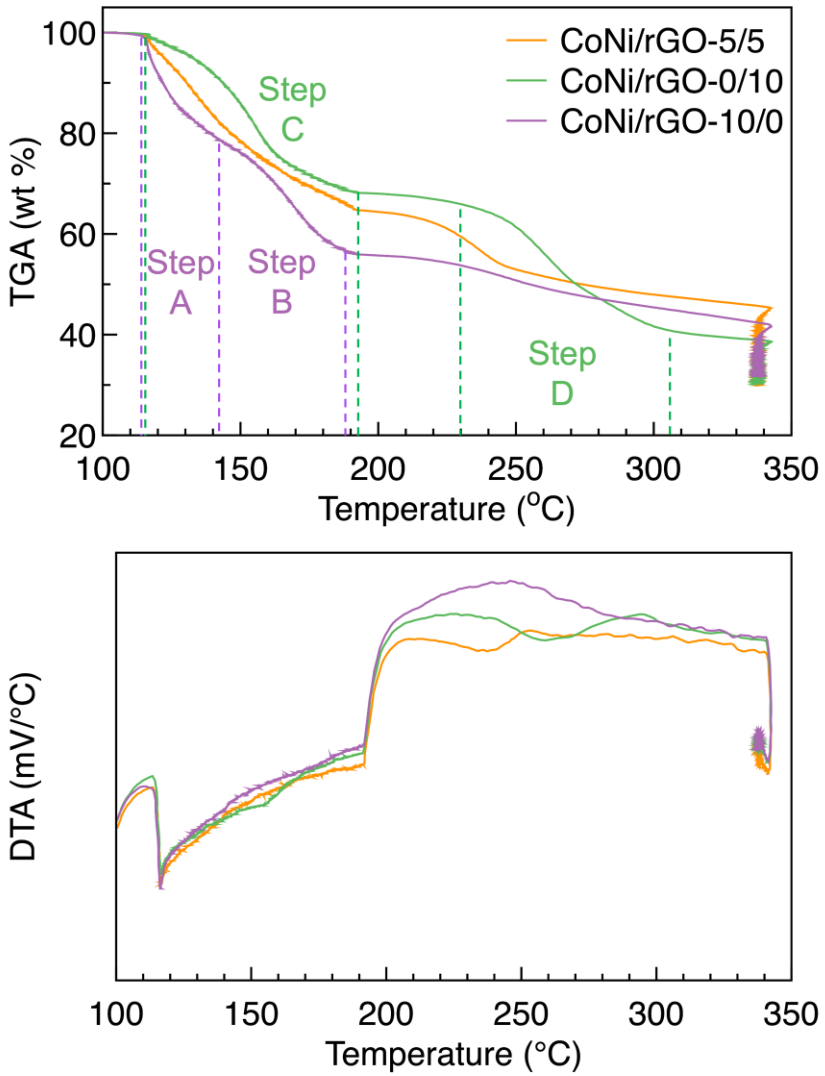

Figure S6. (top) TGA and (bottom) DTA curves of CoNi/rGO-5/5, CoNi/rGO-0/10, and CoNi/rGO-10/0.

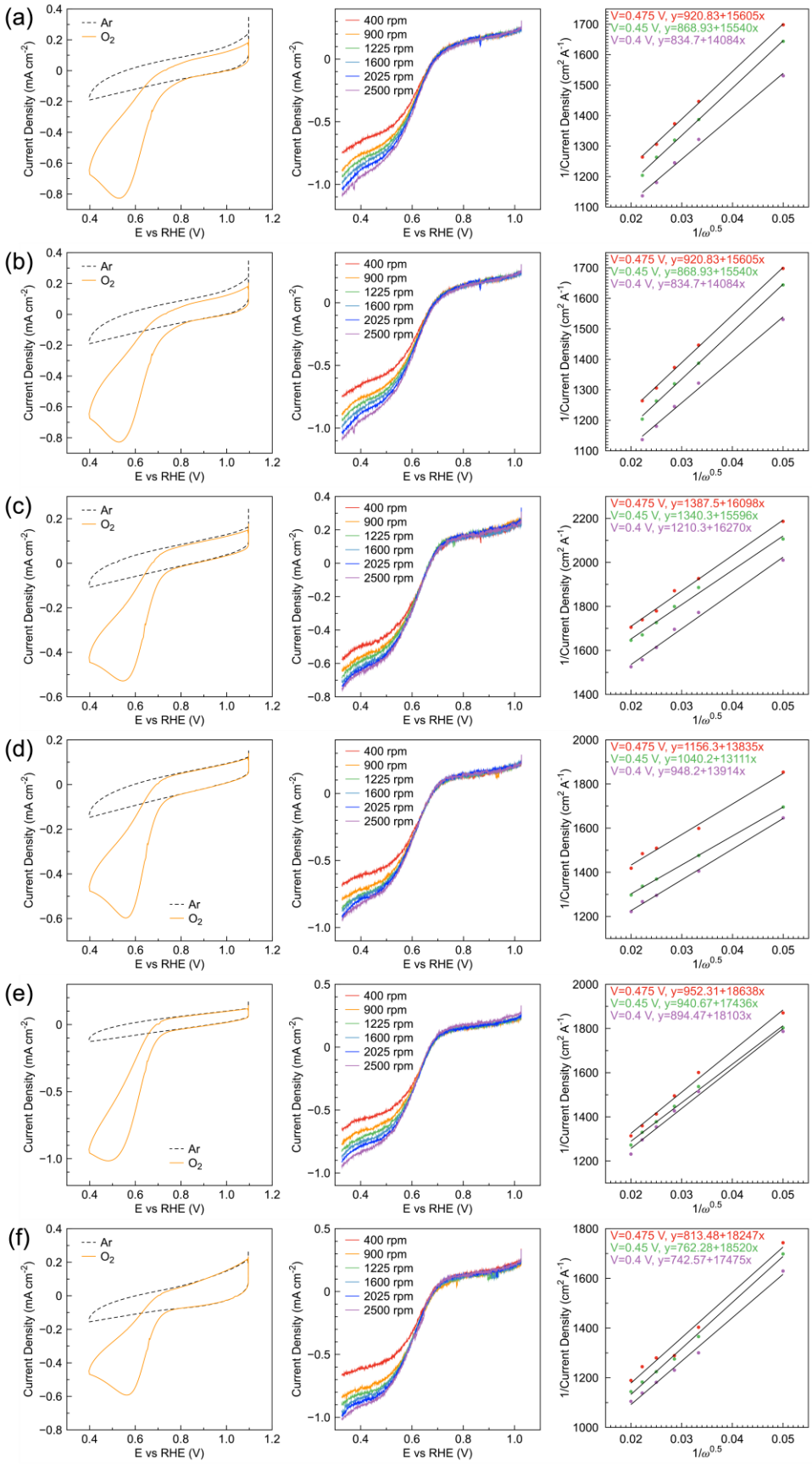

Figure S7. Summary of CV, LSV, and K-L plots of CoNi/rGO-i/j with i/j = (a) 10/0, (b) 8/2, (c) 6/4, (d) 4/6, (e) 2/8, and (f) 0/10.

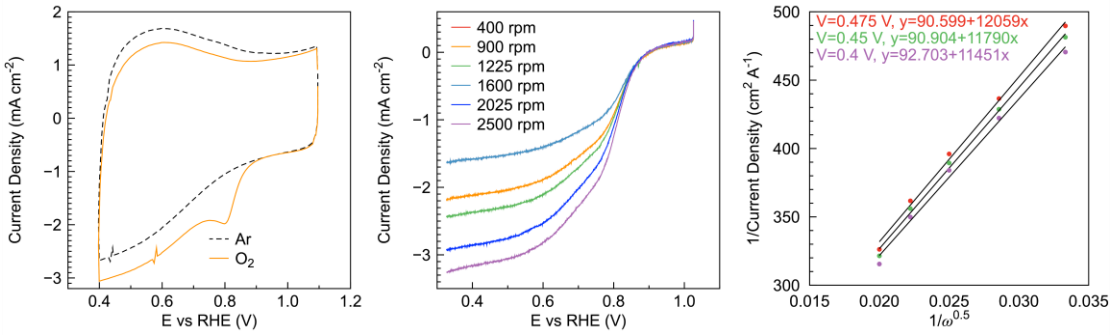

Figure S8. CV, LSV and K-L plots of commercial Pt/C reference catalyst.

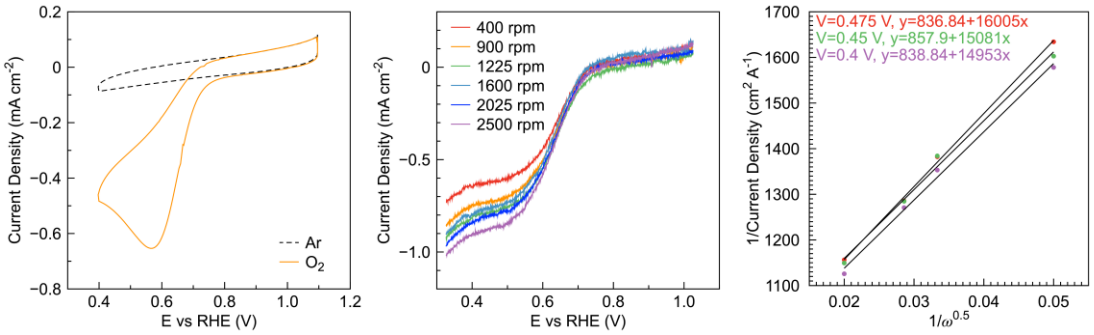

Figure S9. CV, LSV and K-L plots of CoNiMix/rGO catalyst.

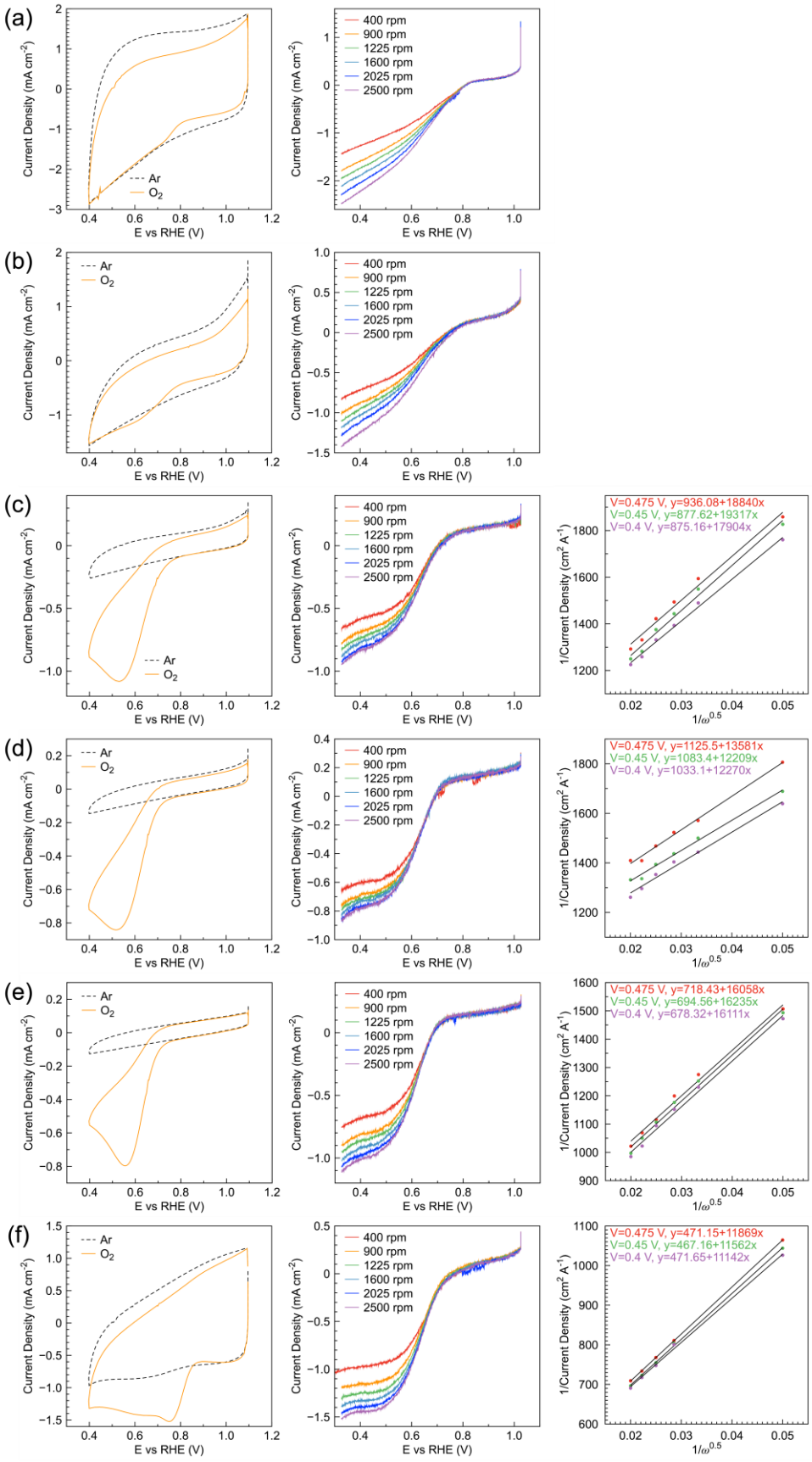

Figure S10. CV, LSV, and K-L plots of CoNi/rGO-w wt% with w = (a) 0 wt%, (b) 20 wt%, (c) 40 wt%, (d) 60 wt%, (e) 80 wt%, and (f) 100 wt%.

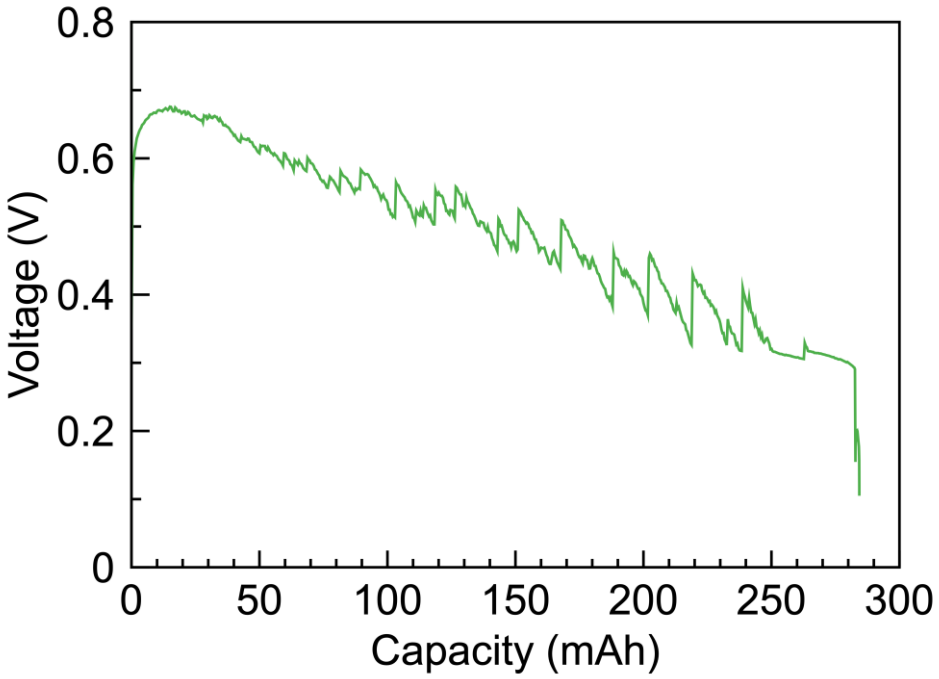

Figure S11. Discharge profile of ZAB with CoNi/rGO-5/5 catalyst for the air electrode at 100 mA·cm^{-2}. The discharge voltage (vs. Zn anode) was more than 0.6 V during the first 1 h discharge.

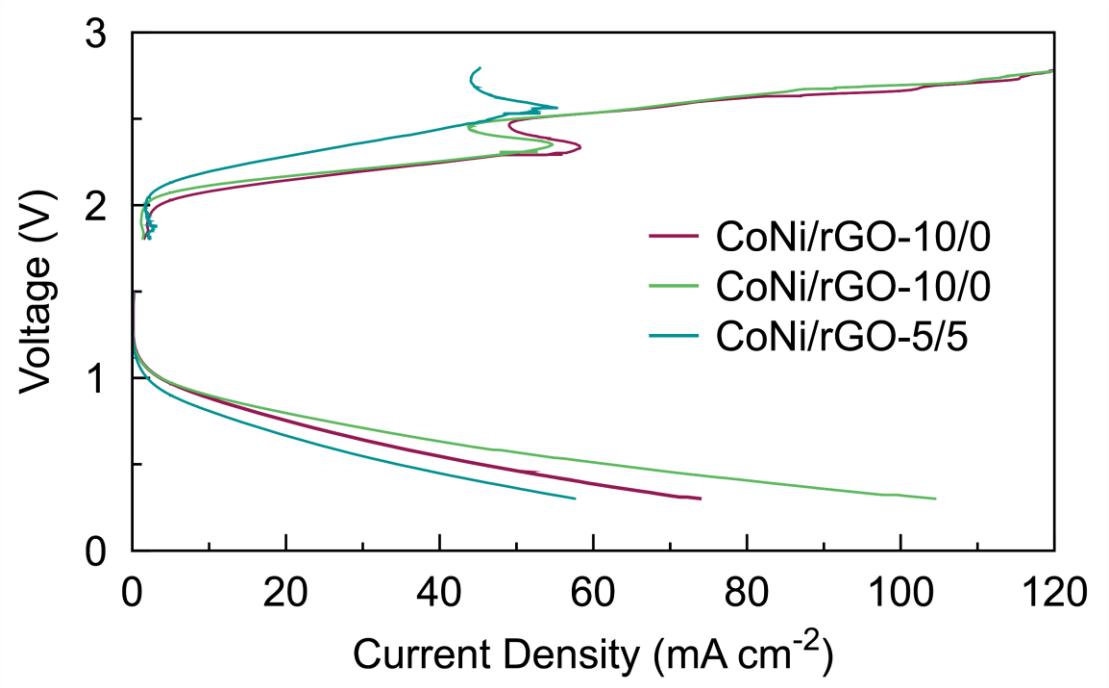

Figure S12. Charge and discharge polarization curves for ZAB using CoNi/rGO-10/0, 5/5, and 0/10 catalysts.

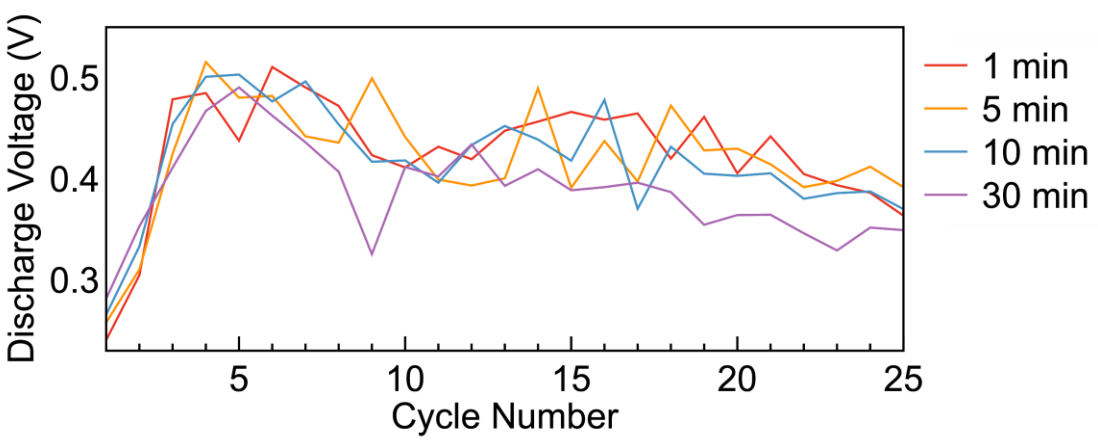

Figure S13. Discharge voltage using CoNi/rGO-5/5 over cycles at 1, 5, 10, and 30 min of discharging process in cycle test of ZABs.

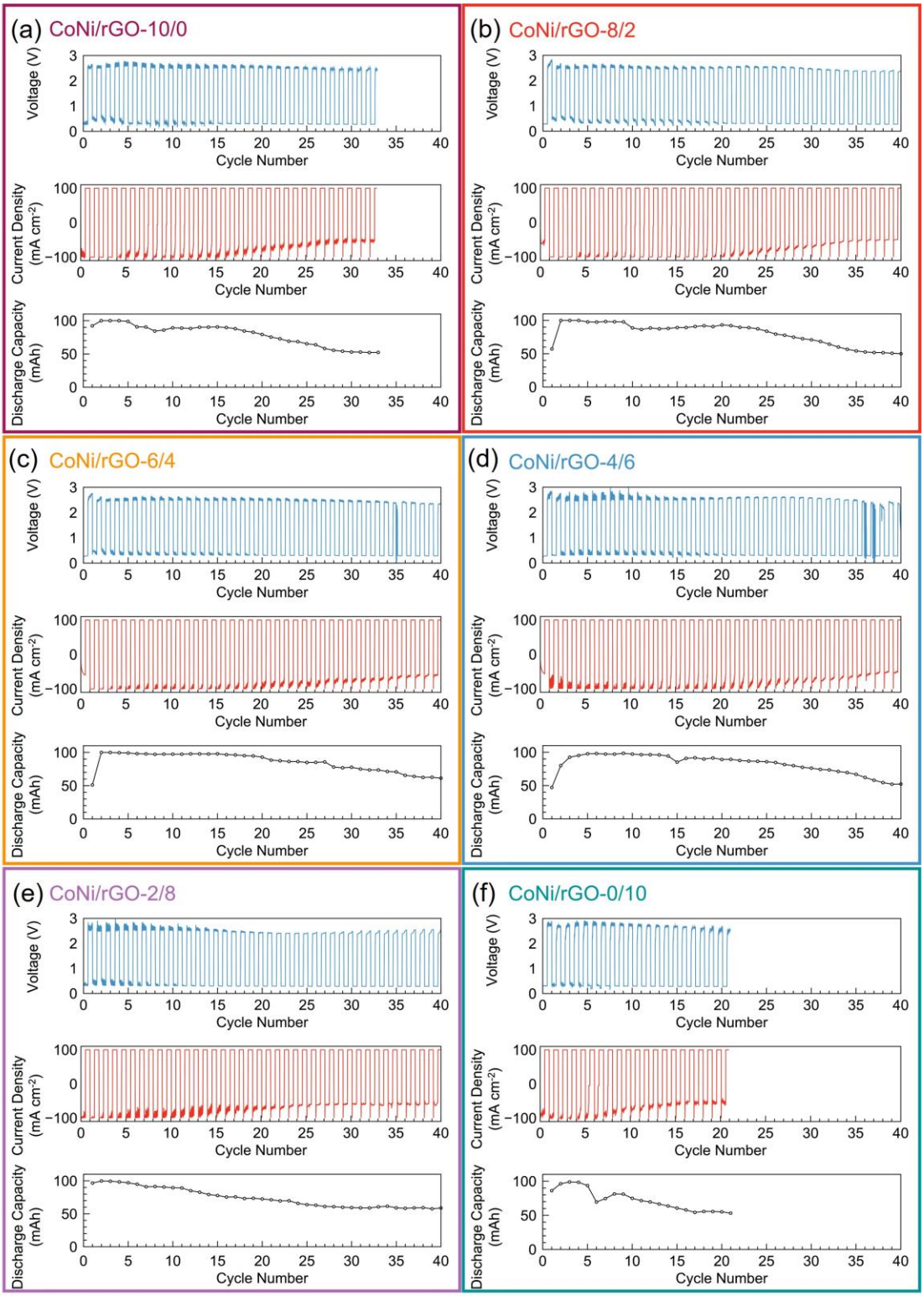

Figure S14. Discharge-charge cycle test results of ZABs at 100 mA·cm^{-2} using CoNi/rGO-i/j with Co:Ni = (a) 10/0, (b) 8/2, (c) 6/4, (d) 4/6, (e) 2/8, and (f) 0/10 (mol/mol).

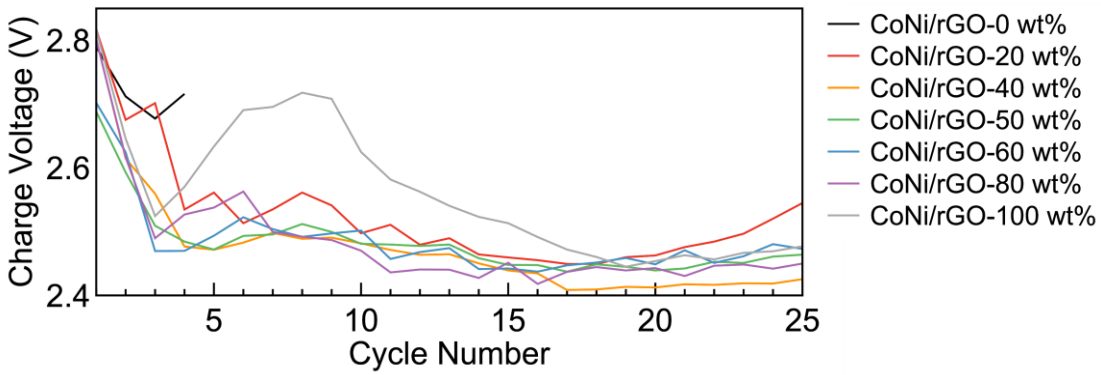

Figure S15. Charging voltage of each discharge-charge cycle in long-term cycle stability test of ZABs using CoNi/rGO catalysts with different metal loading amounts.

References

[1] K. E. Gubbins, J. Robert and D. Walker, *J. Electrochem. Soc.*, **1965**, *112*, 469.
[2] X. Z. Yuan, X. X. Li, W. Qua, D. G. Ivey and H. J. Wang, *ECS Trans*., **2011**, *35*, 11-22.